The kinetic, thermodynamic, and adsorption isotherm analyses of the corrosion inhibition of synthetic extracellular polymeric substances

Liew Chien Go [1], **Dilip Depan** [1], **William Holmes** [2], **August Gallo** [3], **Kathleen Knierim** [3], **Tre Bertrand** [4], **Rafael Hernandez** [Corresp. 1, 2]

[1] Department of Chemical Engineering, University of Louisiana at Lafayette, Lafayette, Louisiana, United States

[2] Energy Institute of Louisiana, University of Louisiana at Lafayette, Lafayette, Louisiana, United States

[3] Department of Chemistry, University of Louisiana at Lafayette, Lafayette, Louisiana, United States

[4] Coastal Chemical Co. LLC, Broussard, Louisiana, United States

Corresponding Author: Rafael Hernandez
Email address: rafael.hernandez@louisiana.edu

Background. Extracellular polymeric substances (EPS) extracted from waste activated sludge (WAS) have previously shown its potential in corrosion inhibition. The aim of this study is to design a synthetic EPS formulation as a surrogate of natural WAS EPS to overcome the corrosion inhibition inconsistency in WAS EPS. The adsorption behavior of the designed inhibitor was studied by kinetic, thermodynamic, and adsorption isotherm analyses.

Methods. Synthetic EPS was formulated based on the typical chemical compositions of natural WAS EPS, i.e. proteins, carbohydrates, humic substances, nucleic acids, and uronic acids. It is a mixture of glutamic acid, carboxymethylcellulose, humic acid, thymine, and alginic acid. Its corrosion inhibition performance was tested with carbon steel in 3.64% NaCl saturated with CO_2, using the potentiodynamic polarization scanning technique. The corrosion kinetic parameters were evaluated using Arrhenius relationships while the thermodynamic adsorption parameters were examined using the Langmuir isotherm and Van't Hoff plot.

Results. The inhibition efficiency improved with increasing inhibitor concentration and temperature. The optimum performance was 94% with 204 mg/L of inhibitor applied at 70°C. The inhibition performance was controlled by both the concentration of inhibitor and temperature. Chemisorption of the inhibitor molecules contributed to the overall inhibition performance by adhering to Langmuir isotherm, deducing that the synthetic EPS formed a monolayer of protection film on the metal surface, reducing the contact of metal with the corrosive environment, thus, slowing down the overall corrosion rate.

The kinetic, thermodynamic, and adsorption isotherm analyses of the corrosion inhibition of synthetic extracellular polymeric substances

Liew Chien Go[1], Dilip Depan[1], William Holmes[2], August Gallo[3], Kathleen Knierim[3], Tre Bertrand[4], Rafael Hernandez[1,2]

[1] Chemical Engineering, University of Louisiana at Lafayette, Lafayette, LA, USA
[2] Energy Institute of Louisiana, University of Louisiana at Lafayette, Lafayette, LA, USA
[3] Chemistry, University of Louisiana at Lafayette, Lafayette, LA, USA
[4] Coastal Chemical Co., LLC, Broussard, LA, USA

Corresponding Author:
Rafael Hernandez[1,2]
131 Rex Street, Lafayette, LA, 70503, USA
Email address: rafael.hernandez@louisiana.edu

Abstract

Background. Extracellular polymeric substances (EPS) extracted from waste activated sludge (WAS) have previously shown its potential in corrosion inhibition. The aim of this study is to design a synthetic EPS formulation as a surrogate of natural WAS EPS to overcome the corrosion inhibition inconsistency in WAS EPS. The adsorption behavior of the designed inhibitor was studied by kinetic, thermodynamic, and adsorption isotherm analyses.

Methods. Synthetic EPS was formulated based on the typical chemical compositions of natural WAS EPS, i.e. proteins, carbohydrates, humic substances, nucleic acids, and uronic acids. It is a mixture of glutamic acid, carboxymethylcellulose, humic acid, thymine, and alginic acid. Its corrosion inhibition performance was tested with carbon steel in 3.64% NaCl saturated with CO_2, using the potentiodynamic polarization scanning technique. The corrosion kinetic parameters were evaluated using Arrhenius relationships while the thermodynamic adsorption parameters were examined using the Langmuir isotherm and Van't Hoff plot.

Results. The inhibition efficiency improved with increasing inhibitor concentration and temperature. The optimum performance was 94% with 204 mg/L of inhibitor applied at 70°C. The inhibition performance was controlled by both the concentration of inhibitor and temperature. Chemisorption of the inhibitor molecules contributed to the overall inhibition performance by adhering to Langmuir isotherm, deducing that the synthetic EPS formed a monolayer of protection film on the metal surface, reducing the contact of metal with the corrosive environment, thus, slowing down the overall corrosion rate.

Introduction

Extracellular polymeric substances (EPS) are the metabolic products produced by most microorganisms. They accumulate on the surface of microorganisms, acting as protective barriers against the microorganisms' external environment [1]. Typically, carbohydrates have been identified as the major constituents in the EPS of many pure cultures [2][3], whereas proteins were found in substantial quantities in the sludge of many wastewater treatment reactors [1][4]. Small amounts of humic substances [5], uronic acids, and nucleic acids [1][6][7] were also detected in EPS. A previous study [8] showed the potential of EPS extracted from waste activated sludge (WAS) of wastewater treatment operations as a green corrosion inhibitor for CO_2 corrosion. A maximum inhibition performance of about 80% was achieved with the application of 1000 mg/L of this inhibitor. The corrosion inhibition mechanism of WAS EPS was explained by the formation of a biofilm on the metal surface, shielding the metal surface from the corrosive environment. Even though the inhibition performance is comparable to commercial products, the nature of WAS caused inconsistency in inhibition efficiency. The composition of WAS is dependent on wastewater treatment operational parameters, such as inlet biochemical oxygen demand and sludge residence time.

This study focused on the evaluation of a corrosion inhibitor from the surrogate of WAS EPS. The reason of making the surrogate was to have control on the chemical composition of the corrosion inhibitor used and ensure consistent inhibition performance. This study hypothesized

that the designed synthetic EPS will demonstrate similar corrosion inhibition behavior as the natural WAS EPS because it was formulated based on the major chemical compositions of natural WAS EPS. The novelty of this research was the design of a surrogate biomass-based corrosion inhibitor inspired by sources with varied chemical compositions. To the knowledge of the authors, this line of work has not been reported elsewhere. The present study seeks to investigate the corrosion inhibitive properties of synthetic EPS for carbon steel in 3.64% NaCl solution saturated with CO_2 gas using the potentiodynamic polarization technique. The corrosion kinetic parameters and thermodynamic adsorption parameters are calculated and reported.

Materials & Methods

Metal specimen preparation

Potentiodynamic polarization scans were performed on carbon steels of the following weight percentage composition: 0.17 C, 0.08 Mn, 0.014 P, 0.002 S, 0.022 Si, 0.02 Cu, 0.01 Ni, 0.04 Cr, 0.002 Sn, 0.042 Al, 0.006 N, 0.001 V, 0.0001 B, 0.001 Ti, 0.001 Cb, and the remainder iron. The pre-treatment of the specimens' surface was carried out by grinding with sandpapers of 40, 220, 320 grits, rinsing with deionized water, then drying with paper towel. The specimens were used immediately after pre-treatment.

Corrosive medium preparation

The corrosive medium was prepared with 36.4 g of NaCl (Fisher Scientific, Hampton, NH, USA) in 1 L of deionized water to make up 3.64% of NaCl solution. The deionized water used was drinking water filtered with Milli-Di Water Purification System (Merck Millipore, Burlington, MA). Prior to starting of each experiment, CO_2 gas was sparged in the test solution at 30 psi for 30 minutes. Then, the solution was transferred into the reactor, with CO_2 gas continuously sparging throughout the experiment at 20 psi.

Corrosion inhibitor preparation

A mixture of several chemical compounds was labelled as synthetic EPS. It was used as the test corrosion inhibitor in this study. The details of each compound, i.e. chemical type, compound identity, vendor, specification, and composition, are listed in Table 1. These compounds were mixed in the given composition as synthetic EPS. The concentrations of inhibitors used in the following runs were doubled, tripled, and quadrupled.

Potentiodynamic polarization method

Potentiodynamic polarization experiments were carried out with Gamry Flexcell Critical Pitting Cell Kit, connecting to the Gamry Potentiostat Interface 1000. The reference, counter, and working electrodes used were saturated calomel electrode (SCE), graphite rod, and the metal specimen, respectively. The setup was equipped with a heating jacket connected to TDC4 Omega temperature controller to maintain the test solution at a desired temperature, in this case, 25°C, 50°C, and 70°C. The Glas-Col GT Series stirrer was connected to the setup externally and adjusted to 50 rpm to get the desired shear and to ensure even heating. The working solution volume was 1 L. The working area of the metal specimens had a circular form of 5 cm^2.

The potentiodynamic polarization scans were carried out in potential range of -0.25 to +0.25 V versus corrosion potential (E_{corr}) at a scan rate of 3 V/hr. Corrosive medium was added into the reactor with carbon dioxide gas sparging constantly at 20 psi throughout the experiment.

The reactor was allowed to equalize for 30 minutes prior to the beginning of experiment. After the system was equalized, Tafel plots were graphed with Gamry DC105 DC Corrosion Technique Software until three relatively similar readings were obtained. Next, corrosion inhibitor was added into the reactor. The reactor was again allowed to equalize for 30 minutes, then Tafel plots were graphed. This step was repeated until three consecutive graphs with similar trends were yielded, to ensure the stability of the system. Subsequently, the concentration of the corrosion inhibitor was increased. Again, the system was being equalized for 30 minutes, followed by the graphing of Tafel plots.

The Tafel plot was plotted with the mean values of corrosion potential (E_{corr}) and corrosion current density (I_{corr}) from the triplicates of the experiments, while the electrochemical parameters obtained from the curves were reported with mean and standard deviation. The corrosion current densities were found by extrapolating the linear Tafel segment of the anodic and cathodic curves to the corrosion potential. The corrosion inhibition efficiency was then calculated with Equation 1.

$$Inhibition\ Efficiecny\ (\%) = \frac{I_{corr,\ uninhibited} - I_{corr,\ inhibited}}{I_{corr,\ uninhibited}} \times 100\% \quad (1)$$

Fourier-transform infrared spectroscopy (FTIR)

Agilent Cary 630 FTIR incorporated with MicroLab software were used for the FTIR analysis in this study. This equipment worked based on Attenuated Total Reflection (ATR) Method. The scanning was range between 4000 to 400 cm^{-1} with resolution of 4 cm^{-1}.

Results

Corrosion inhibition performance

The Tafel plots generated from the potentiodynamic polarization measurements for carbon steel in 3.64% NaCl saturated with CO_2 gas with synthetic EPS range from 51 mg/L to 204 mg/L at 25°C, 50°C, and 70°C are presented in Figure 1, Figure 2, and Figure 3, respectively. The details of electrochemical parameters obtained from the curves, namely corrosion potential (E_{corr}), corrosion current density (I_{corr}), and inhibition efficiency, are listed in Table 2.

Corrosion kinetic parameters

Corrosion kinetic parameters, i.e. apparent activation corrosion energy (E_a), enthalpy of activation ($\Delta H_a°$), and entropy of activation ($\Delta S_a°$), are listed in Table 3. Two Arrhenius plots are shown in Figure 4 and Figure 5.

Thermodynamic adsorption parameters

The standard free energy of adsorption ($\Delta G°_{ads}$), enthalpy of adsorption ($\Delta H_{ads}°$), and the entropy of adsorption ($\Delta S_{ads}°$) are listed in Table 4. The Langmuir isotherm and the Van't Hoff plots are shown in Figure 6 and Figure 7, respectively.

FTIR

The IR spectra is shown in Figure 8 **Error! Reference source not found.**and the characteristic IR absorption frequencies of the responding organic functional groups of synthetic EPS is tabulated in Table 5.

Discussion

Properties of synthetic EPS

Synthetic EPS is a mixture of several major groups of chemicals in natural WAS EPS. Although there are many ways to extract EPS and each of the methods give different chemical composition [1][9][7]; the composition of synthetic EPS formulated in this study will be based on the method of heating. Typically, the EPS extracted by heating has the highest proteins concentration, followed by carbohydrates, humic substances, nucleic acids, and uronic acids [1][9][7]. Therefore, proteins will be the basis of the synthetic EPS and the ratio of different chemicals will be based on the proteins. The compounds were mixed in ratios that were realistic (small enough concentration to be able to measured accurately using an analytical balance) to be acted as a corrosion inhibitor. They were mixed according to the following ratios:

a. Proteins:carbohydrates = 2.5:1
b. Proteins:humic substances = 6:1
c. Proteins:nucleic acids = 15:1
d. Proteins:uronic acids =15:1

One compound was selected from each chemical group. They were chosen based on their structures and their chemical inhibition performances in the literature. Structure wise, compounds with nitrogen, oxygen, or sulfur atoms were preferred since all organic corrosion inhibitors typically contain at least one of these atoms, almost without exception. Furthermore, those chemicals that had demonstrated corrosion inhibition were prioritized to be the candidates in the pool of selection. For protein, an amino acid, which is the building block of a protein was chosen. Glutamic acid, a common component of bacterial cell wall [10], made an excellent candidate as an amino acid for the purpose of this study because it has been proven to be an effective corrosion inhibitor in several studies [11][12], so, it was chosen as the main component of the synthetic EPS. The second biggest composition was carbohydrate. For an organic corrosion inhibitor, typically, a bigger molecule is preferred. Carboxymethylcellulose (CMC), a relatively big molecular weight packed with multiple oxygen atoms, was selected as the candidate for the chemical group of carbohydrate. Its corrosion inhibition capability has also been proven excellent in various investigations [13][14]. However, corrosion inhibition studies on the rest of the chemical groups have no record in the literature to date. For humic substances and uronic acids, there are not many chemicals from these groups, so, humic acid and alginic acid were picked for each group, respectively. In the case of nucleic acids, there are only four choices in this group, namely thymine, guanine, adenine, and cytosine. Making a decision based on an economical point of view, the most affordable choice was thymine. Thymine is a relatively smaller compound compared to other chosen chemicals, but it contains both nitrogen and oxygen atoms, making it a desirable option. Hence, glutamic acid, CMC, humic acid, thymine, and alginic acid were chosen as the formulation for synthetic EPS. Their chemical structures are shown in Figure 9.

Effect of concentration

The curves in Figure 1, Figure 2, and Figure 3 revealed well defined anodic and cathodic polarization Tafel regions. As observed in these figures, both cathodic and anodic reactions of carbon steel electrode corrosion were inhibited by the increase concentration of synthetic EPS in 3.64% NaCl saturated with CO_2 gas. This observation indicates that the addition of synthetic

EPS reduced anodic dissolution as well as the hydrogen evolution reaction [15]. This can be explained by the adsorption of inhibitor over the corroded surface [16]. Tafel lines of nearly equal slopes were obtained, indicating that the hydrogen evolution reaction was activated-controlled [17].

The details of electrochemical parameters obtained from the Tafel plots such as the values of corrosion potential, E_{corr}, corrosion current density, I_{corr}, corrosion protection efficiency, and surface coverage degree, θ, are presented in Table 2. The corrosion inhibition efficiency was calculated using Equation 1, based on the I_{corr} values, where $I_{corr,blank}$ and I_{corr} were the corrosion current density without and with inhibitor, respectively. These values were obtained by the extrapolation of the cathodic and anodic Tafel lines to the corrosion potentials. The data showed that the I_{corr} values decreased in the presence of synthetic EPS. These values also dropped as the concentration of inhibitor increased, meaning that the corrosion reaction was slowing down as the inhibitor concentration was increasing. This phenomenon can be attributed to the adsorption of synthetic EPS on the metal surface [17].

There was no definite pattern observed in E_{corr} values in the presence of different concentrations of synthetic EPS. This result indicated that synthetic EPS may be considered as a mixed-type corrosion inhibitor [18] in the presence of CO_2 gas saturated 3.64% NaCl solution. The maximum displacement in E_{corr} of less than 0.085 V suggests a mixed mode of inhibition [19]. Mixed-type corrosion inhibitor retards corrosion rate by suppressing both anodic and cathodic corrosion reactions, typically by adsorbing on a metal surface, forming a protective film to reduce contact of metal surface from the corrosive environment [20].

The inhibition efficiency increased as the concentration of synthetic EPS increased. The maximum inhibition was about 94% with an optimum inhibitor concentration of 204 mg/L at 70°C. At 25°C, the maximum inhibition protection of synthetic EPS was 82% at a concentration of 153 mg/L. The previous study of WAS EPS inhibitor demonstrated an optimum inhibition performance of about 79% at a concentration of 1000 mg/L [8]. Even though the inhibition performance showed only a mere improvement of 3%, the inhibitor concentration was reduced by about 6.5 times. It is known that the natural WAS EPS is rich in a variety of compounds. These compounds could have posed stearic hindrance on the adsorption of inhibition molecules on the metal surface, bring down the efficiency of the overall inhibition performance, so, higher concentrations of inhibitors were required to demonstrate the corrosion inhibition capability. Unlike the natural WAS EPS, the synthetic EPS was formulated specifically on the EPS groups that are known to perform as corrosion inhibitors. Hence, it is expected that the corrosion inhibition efficiency of synthetic EPS to be higher than the natural WAS EPS. Furthermore, in the case of commercial corrosion inhibitors, their corrosion protection performances are typically above 70%. Synthetic EPS has a corrosion inhibition performance that is within the range of commercial corrosion inhibitors. One advantage compared to natural WAS EPS is that its inhibition performance is consistent. The results obtained from this study strongly suggest the great potential commercialization value of synthetic EPS as a valuable material to inhibit corrosion issues in oilfield operations.

Effect of temperature

The effect of temperature on the inhibited solution–metal reaction is highly complex because many changes could occur on the metal surface such as rapid etching and desorption of inhibitor, also, the inhibitor itself may undergo decomposition and/or rearrangement [21]. The effect of corrosion inhibition by synthetic EPS in NaCl solution saturated with CO_2 gas was

studied with three different temperatures, i.e. 25°C, 50°C, and 70°C. Since the corrosion rate is greatly affected by the concentration of inhibitor as well as the temperature of the working environment, these factors have an important operational impact.

At different temperatures and inhibitor concentrations, the corrosion inhibition efficiencies varied. It was apparent that the rates of carbon steel corrosion, both in the blank solution of 3.64% NaCl saturated with CO_2 gas and with the presence of corrosion inhibitor, increased with increasing temperature. The impact of temperature on the overall corrosion reaction was more pronounced than the effect of inhibitor concentration. The inhibition efficiency increased with temperature. Typically, a decrease in inhibition efficiency with a rise in temperature suggests physisorption of the corrosion inhibitor. In contrast, an increase in inhibition efficiency with rise in temperature is indicative of a a chemisorption mechanism [22]. Therefore, the results clearly indicate a chemisorption mechanism of synthetic EPS on the carbon steel surface.

Corrosion kinetic parameters

The activation parameters for the corrosion reaction were calculated using an Arrhenius-type plot according to Equation 2. E_a in the equation denotes the apparent activation corrosion energy, R is the universal gas constant, and k is the Arrhenius pre-exponential factor. The values of apparent activation energy of corrosion were determined from the slope of ln I_{corr} versus 1/T plot, shown in Figure 4. The data showed lower activation energy in the presence of inhibitors than in its absence, which is a typical pattern of chemisorption [17].

An alternative formulation of Arrhenius equation, i.e. transition-state equation shown in Equation 3, was used to calculate the change of enthalpy ($\Delta H_a°$) and entropy ($\Delta S_a°$) of activation for the activation complex formation in the transition state. In this equation, the h is the Planck's constant, N is the Avagadro's number, $\Delta S_a°$ is the entropy of activation, and $\Delta H_a°$ is the enthalpy of activation. Figure 5 shows a plot of ln (I_{corr}/T) against 1/T for synthetic EPS. A straight line was obtained with a slope of $\Delta H_a°/R$ and an intercept of ln (R/Nh + $\Delta S_a°$/R), from which the values of $\Delta H_a°$ and $\Delta S_a°$ were calculated. The positive enthalpy values reflected the endothermic nature of metal dissolution process. Large and negative values of entropy imply that the activated complex in the rate determining step represents an association rather than a dissociation step [17].

$$I_{corr} = ke^{-\frac{E_a}{RT}} \quad (2)$$

$$I_{corr} = \frac{RT}{Nh} exp\left(\frac{\Delta S_a^0}{R}\right) exp\left(-\frac{\Delta H_a^0}{RT}\right) \quad (3)$$

Thermodynamic adsorption parameters

Adsorption isotherms provide insights into the interaction among the adsorbed molecules and the metal surface, which can help to better understand the corrosion inhibition mechanism. The values of surface coverage (θ) to different concentrations of inhibitor, obtained from the polarization measurements in the temperature range of 25 to 70°C were used to explain the best isotherm to determine the adsorption mechanism. The values of θ were assumed to be the corrosion inhibition efficiencies. They were used in a series of equations shown in Equation 4, Equation 5, and Equation 6 [23]. Equation 4 showed the relationship of I_{corr}, $I_{corr,blank}$, I_{sat}, and θ. I_{sat} is the current density of entirely covered surface. This equation was then be rearranged into Equation 5. As I_{corr} was greater than I_{sat}, Equation 5 was simplified to Equation 6.

$$I_{corr} = (1 - \theta) I_{corr,blank} + \theta I_{sat} \quad (4)$$

$$\theta = \frac{I_{corr,\,blank} - I_{corr}}{I_{corr,blank} - I_{sat}} \quad (5)$$

$$\theta = \frac{I_{corr,\,blank} - I_{corr}}{I_{corr,blank}} \quad (6)$$

In the range of temperature and inhibitor concentration studied, the best correlation between the experimental results and the adsorption isotherm functions was obtained using Langmuir adsorption isotherm. The Langmuir isotherm for monolayer adsorption is given by Equation 7. By linearizing this equation, Equation 8 was obtained.

$$\frac{\theta}{1 - \theta} = KC \quad (7) \qquad \frac{C}{\theta} = \frac{1}{K} + C \quad (8)$$

In Equation 7 and Equation 8, θ is the surface coverage degree, C is the inhibitor concentration in the NaCl solution, and K is the equilibrium constant of the adsorption process. The correlation coefficient, R^2, was used to describe how close the isotherm fits the experimental data. The plot of C/θ against C gave a straight line and the linear correlation coefficients were fairly close to 1, indicating good fit to the data. This graph is shown in Figure 6. The adsorption behavior of synthetic EPS conformed to Langmuir isotherm, suggesting monolayer adsorption, which is a typical behavior of chemisorption [24].

K values were calculated from the intercepts of the same plot (Figure 6). The constant of adsorption, K, can be related to the standard free energy of adsorption, $\Delta G°_{ads}$, using Equation 9. The constant 1 x 10^6 in the equation is the concentration of water molecules expressed in mg/L, R is the universal gas constant, T is the absolute temperature. On the other hand, $\Delta H°_{ads}$ can be deduced from the integrated version of the Van't Hoff equation expressed by Equation 10**Error! Reference source not found.**. Figure 7 shows the plot of ln K versus 1/T which yield a straight line with a slope of $-\Delta H°_{ads}/R$. The value obtained was used to find the $\Delta H°_{ads}$. The calculated $\Delta H°_{ads}$ was then used to calculate the values of $\Delta S°_{ads}$ by using Equation 11.

$$\Delta G^{\circ}_{ads} = - RT ln\,(1 \times 10^6\, K) \quad (9)$$

$$ln\, K = - \frac{\Delta H^{\circ}_{ads}}{RT} + \frac{\Delta S^{\circ}_{ads}}{R} \quad (10)$$

$$\Delta G^{\circ}_{ads} = \Delta H^{\circ}_{ads} - T \Delta S^{\circ}_{ads} \quad (11)$$

A more in-depth study of the inhibitor adsorption mechanism was investigated using the values of thermodynamic parameters. The details can be found in Table 4. The spontaneity of the adsorption of inhibitor on the metal surface as well as the stability of the adsorbed layer on the metal surface was demonstrated by the resulted negative values of $\Delta G°_{ads}$. Typically, an endothermic adsorption process that has a positive value of $\Delta H°_{ads}$ is attributed unequivocally to chemisorption, while an exothermic adsorption process with $\Delta H°_{ads}$ of negative value may involve either physisorption or chemisorption, or a combination of both the processes [21]. In this study, the $\Delta H°_{ads}$ was positive, once again implying a chemisorption mechanism. The value of $\Delta S°_{ads}$ decreased with increased temperature, implying that the reaction of adsorption was getting less disordered.

FTIR

The trend in the IR spectrum of the synthetic EPS followed closely to the natural WAS EPS [8] as expected because it is formulated based on the chemical composition of natural WAS EPS. Similar to the natural WAS EPS, the FTIR results of synthetic EPS showed that functional

groups O-H, N-H, C-N, C=O, and C-H were present. Since the synthetic EPS and natural WAS EPS both have the same functional group, it can be deduced that these functional groups play major roles in corrosion inhibition.

The electrochemical theory of corrosion holds that the metal surface corroding in an electrolyte is covered with local electrolytic cells. Some areas of the metal can act as anodes and other areas can act as cathodes, depending upon the history of the metal regarding heat treatment, presence of imperfections, scratches, greases, paint coatings, fingerprint smudges, etc. At anodic sites, the metal usually dissolves into solution. Electrons given from these sites are transported to local cathodes and collected by electron acceptors such as hydrogen ions and oxygen. As previously suggested, synthetic EPS acts as a mixed-type corrosion inhibitor, meaning that the molecules in the synthetic EPS chemisorbed on both the anodic and cathodic sites of metal surface to form a monolayer protection film. The functional groups rich in nitrogen and oxygen atoms acted as the polar head of organic corrosion inhibitors, adsorbing on metal surface by forming chemical bonds between the inhibitor molecules and metal ions, while the non-polar hydrocarbon chain attached to the polar head isolated the metal surface from the corrosive surrounding, suppressing both anodic and cathodic corrosion reactions, reducing the overall corrosion rate.

Conclusions

The studied inhibitor, synthetic EPS, is a surrogate of biomass-based corrosion inhibitor inspired by sources with varied chemical compositions to overcome the composition inconsistency in biomass that can cause unreliable corrosion inhibition performance. Synthetic EPS is a mixture of glutamic acid, carboxymethylcellulose, humic acid, thymine, and alginic acid, following the chemical composition of natural WAS EPS extracted by heating method. Unlike the natural WAS EPS that is rich in assorted of molecules that could promote stearic hindrance on the adsorption of inhibitor molecules, synthetic EPS was designed specifically based on the EPS groups that are known to perform as corrosion inhibitors. With concentration of 204 mg/L in 3.64% NaCl saturated with CO_2 gas, synthetic EPS showed maximum corrosion inhibitions of 82.41%, 89.65%, and 93.99% at 25°C, 50°C, and 70°C, respectively. Its performance compared favorably with natural WAS EPS and commercial corrosion inhibitors.

The adsorption mechanism adhered to Langmuir isotherm. It was found that the inhibition performance was controlled by both the concentration of inhibitor and temperature.

The corrosion inhibition capability was due to chemisorption shown by several evidences:

(1) An increase in corrosion inhibition efficiency with increase temperature
(2) A decrease in activation energy in the presence of inhibitor
(3) The adsorption isotherm conforms to the Langmuir monolayer mechanism
(4) Endothermic adsorption

Since the formulation of synthetic EPS was designed solely based on the chemical composition of natural WAS EPS, it was not optimized to meet the purpose of corrosion inhibition. Based on the results presented and the needs and requirements of corrosion protection service providers, the future direction of the current research will focus on optimizing the

formulation in order to reduce the required applied concentration of corrosion inhibitor while achieving the maximum attainable corrosion inhibition performance. This could be done by first reducing the number of compounds in the formulation, then optimizing the concentration of the compounds and the inhibition performance statistically.

References

[1] H. Liu and H. H. P. Fang, "Extraction of extracellular polymeric substances (EPS) of sludges," *J. Biotechnol.*, vol. 95, no. 3, pp. 249–256, 2002.

[2] P. Cescutti, R. Toffanin, P. Pollesello, and I. W. Sutherland, "Structural determination of the acidic exopolysaccharide produced by a Pseudomonas sp. strain 1.15," *Carbohydr. Res.*, vol. 315, no. 1, pp. 159–168, 1999.

[3] L. Kennedy and I. W. Sutherland, "Polysaccharide lyases from gellan-producing Sphingomonas spp.," *Microbiology*, vol. 142, no. 4, pp. 867–872, Apr. 1996.

[4] M. C. Veiga, M. K. Jain, W. Wu, R. I. Hollingsworth, and J. G. Zeikus, "Composition and role of extracellular polymers in methanogenic granules.," *Appl. Environ. Microbiol.*, vol. 63, no. 2, pp. 403–407, 1997.

[5] B. F. Nielsen, T. Griebe, and P. H. Nielsen, "Enzymatic activity in the activated-sludge floc matrix," *Appl. Microbiol. Biotechnol.*, vol. 43, no. 4, pp. 755–761, 1995.

[6] H. JI, "Polymerization of humic substances in natural environments," in *Humic substances and their role in the environment*, Chichester: Wiley, 1988, pp. 45–58.

[7] B. Frølund, R. Palmgren, K. Keiding, and P. H. Nielsen, "Extraction of extracellular polymers from activated sludge using a cation exchange resin," *Water Res.*, vol. 30, no. 8, pp. 1749–1758, 1996.

[8] L. C. Go, W. Holmes, D. Depan, and R. Hernandez, "Evaluation of extracellular polymeric substances extracted from waste activated sludge as a renewable corrosion inhibitor," *PeerJ*, vol. 7, p. e7193, Jun. 2019.

[9] S. Comte, G. Guibaud, and M. Baudu, "Relations between extraction protocols for activated sludge extracellular polymeric substances (EPS) and EPS complexation properties: Part I. Comparison of the efficiency of eight EPS extraction methods," *Enzyme Microb. Technol.*, vol. 38, no. 1, pp. 237–245, 2006.

[10] D. S. Hoare, "the breakdown and biosynthesis of glutamic acid," *J. Gen. Microbiol.*, vol. 32, no. 2, pp. 157–161, Aug. 1963.

[11] D.-Q. Zhang, Q.-R. Cai, L.-X. Gao, and K. Y. Lee, "Effect of serine, threonine and glutamic acid on the corrosion of copper in aerated hydrochloric acid solution," *Corros. Sci.*, vol. 50, no. 12, pp. 3615–3621, 2008.

[12] D.-Q. Zhang, Q.-R. Cai, X.-M. He, L.-X. Gao, and G.-D. Zhou, "Inhibition effect of some amino acids on copper corrosion in HCl solution," *Mater. Chem. Phys.*, vol. 112, no. 2, pp. 353–358, 2008.

[13] M. M. Solomon, S. A. Umoren, I. I. Udosoro, and A. P. Udoh, "Inhibitive and adsorption behaviour of carboxymethyl cellulose on mild steel corrosion in sulphuric acid solution," *Corros. Sci.*, vol. 52, no. 4, pp. 1317–1325, 2010.

[14] E. Bayol, A. Gurten, M. Dursun, and K. Kayakirilmaz, "Adsorption behavior and inhibition corrosion effect of sodium carboxymethyl cellulose on mild steel in acidic medium," *Acta Physico-Chimica Sin.*, vol. 24, no. 12, pp. 2236–2243, Dec. 2008.

[15] M. S. Morad, "Inhibition of phosphoric acid corrosion of zinc by organic onium compounds and their adsorption characteristics," *J. Appl. Electrochem.*, vol. 29, pp. 619–626, 1999.

[16] M. Abdallah, "Guar gum as corrosion inhibitor for carbon steel in sulfuric acid solutions," *Port. Electrochim. Acta*, vol. 22, pp. 161–175, 2004.

[17] M. Bouklah, B. Hammouti, M. Lagrenée, and F. Bentiss, "Thermodynamic properties of 2,5-bis(4-methoxyphenyl)-1,3,4-oxadiazole as a corrosion inhibitor for mild steel in

normal sulfuric acid medium," *Corros. Sci.*, vol. 48, no. 9, pp. 2831–2842, 2006.

[18] Harish Kumar and Vikas Yadav, "Citrus sinensis peels as a Green Corrosion Inhibitor for Mild Steel in 5.0 M Hydrochloric Acid Solution," *Res. J. Chem. Sci.*, vol. 6, no. 1, pp. 53–60, 2016.

[19] N. Chaubey, V. K. Singh, and M. A. Quraishi, "Effect of some peel extracts on the corrosion behavior of aluminum alloy in alkaline medium," *Int. J. Ind. Chem.*, vol. 6, no. 4, pp. 317–328, Nov. 2015.

[20] R. Myrdal, "Corrosion inhibitors– State of the art," 2010.

[21] F. Bentiss, M. Lebrini, and M. Lagrenée, "Thermodynamic characterization of metal dissolution and inhibitor adsorption processes in mild steel/2,5-bis(n-thienyl)-1,3,4-thiadiazoles/hydrochloric acid system," *Corros. Sci.*, vol. 47, no. 12, pp. 2915–2931, 2005.

[22] A. Popova, E. Sokolova, S. Raicheva, and M. Christov, "AC and DC study of the temperature effect on mild steel corrosion in acid media in the presence of benzimidazole derivatives," *Corros. Sci.*, vol. 45, no. 1, pp. 33–58, 2003.

[23] E. Khamis, "The Effect of Temperature on the Acidic Dissolution of steel in the presence of inhibitors," *Corrosion*, vol. 46, no. 6, pp. 476–484, 1990.

[24] "Thermodynamics and Kinetics of Adsorption." [Online]. Available: http://w0.rz-berlin.mpg.de/imprs-cs/download/Vortrag_IMPRS_Schmoeckwitz_Mi_9-11_KChrist.pdf.

Table 1(on next page)

Details of synthetic EPS

Type	Chemical	Vendor	Specification	Amount (mg/L)
Protein	Glutamic acid	Acros Organics	99%	30
Carbohydrate	Carboxymethyl cellulose (CMC)	Acros Organics	MW 70,000	12
Humic acid	Humic acid	Acros Organics	45-70%	5
Nucleic acid	Thymine	Alfa Aesar	97%	2
Uronic acid	Alginic acid, sodium salt	Acros Organics	-	2

1

Table 2(on next page)

Electrochemical parameters and the corresponding corrosion inhibition efficiencies in the presence of different concentrations of synthetic EPS at various temperatures

Temperature (°C)	Concentration (mg/L)	E_{corr} (V)	I_{corr} (μA/cm^2)	Inhibition efficiency (%)	Surface coverage degree, θ
25	0	-0.73	52.48	-	-
	51	-0.71	25.12	68.72	0.69
	102	-0.71	18.20	77.34	0.77
	153	-0.71	14.45	82.00	0.82
	204	-0.70	14.13	82.41	0.82
50	0	-0.74	125.89	-	-
	51	-0.76	37.15	86.03	0.86
	102	-0.76	34.67	86.96	0.87
	153	-0.76	33.11	87.55	0.88
	204	-0.76	27.54	89.65	0.90
70	0	-0.73	223.87	-	-
	51	0.76	45.71	91.70	0.92
	102	-0.76	39.81	92.77	0.93
	153	-0.76	34.67	93.71	0.94
	204	0.75	33.11	93.99	0.94

1

Table 3(on next page)

Corrosion kinetic parameters for carbon steel in different concentrations of the synthetic EPS

Inhibitor concentration (mg/L)	Ea (kJ/mol)	$\Delta H_a°$ (kJ/mol)	$\Delta S_a°$ (J/mol K)
0	27.46	24.81	-71.28
51	12.54	8.75	-131.24
102	15.21	12.56	-120.83
153	17.24	14.59	-115.63
204	16.47	13.82	-118.73

1

Table 4(on next page)

Thermodynamic parameters for the adsorption of synthetic EPS at different temperatures

Temperature (°C)	R^2	K ($[mg/L]^{-1}$)	$\Delta G_{ads}°$ (kJ/mol)	$\Delta H_{ads}°$ (kJ/mol)	$\Delta S_{ads}°$ (J/mol K)
25	0.9980	0.01	-22.93	7.5192	102.11
50	0.9969	0.01	-23.53		72.81
70	0.9999	0.02	-23.91		69.68

1

Table 5(on next page)

Characteristic IR absorption frequencies of organic functional groups

Characteristic Absorptions (cm^{-1})	Vibration Type	Functional Type
3,200 - 3,600	Phenol OH stretch	OH into polymeric compounds
2,850 - 3,000	Alkane C-H stretch	
1,690 - 1,630	Amide C=O stretch	Proteins
1,590 - 1,650	Amide (I) N-H bend	
1,500 - 1,560	Amide (II) N-H bend	
1,350 - 1,480	Alkane C-H bending	
1,080 - 1,360	Amine C-N stretch	

1

Figure 1

Tafel plot for carbon steel in 3.64% NaCl concentrated with CO_2 with different concentrations of synthetic EPS at 25°C

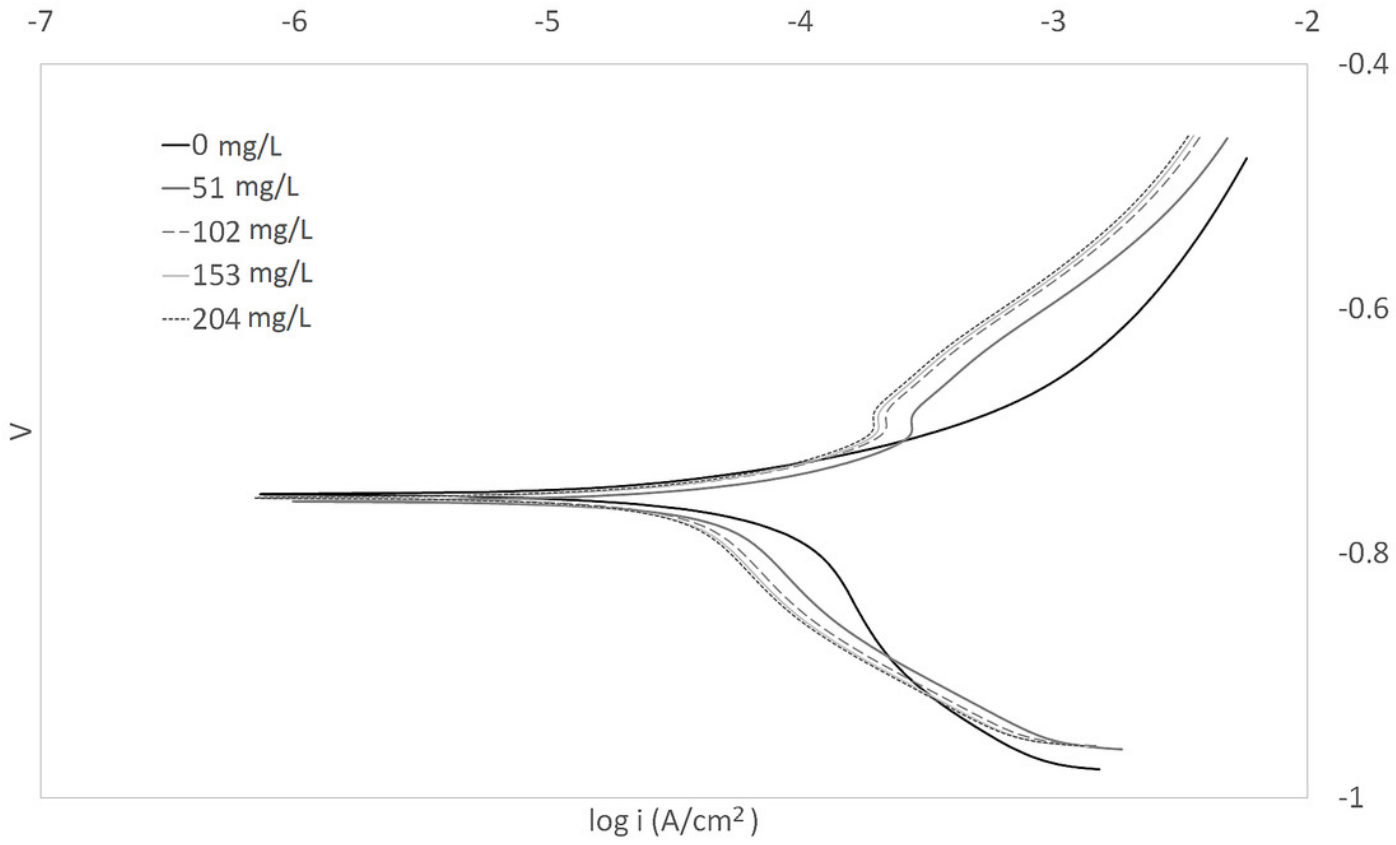

Figure 2

Tafel plot for carbon steel in 3.64% NaCl concentrated with CO_2 with different concentrations of synthetic EPS at 50°C

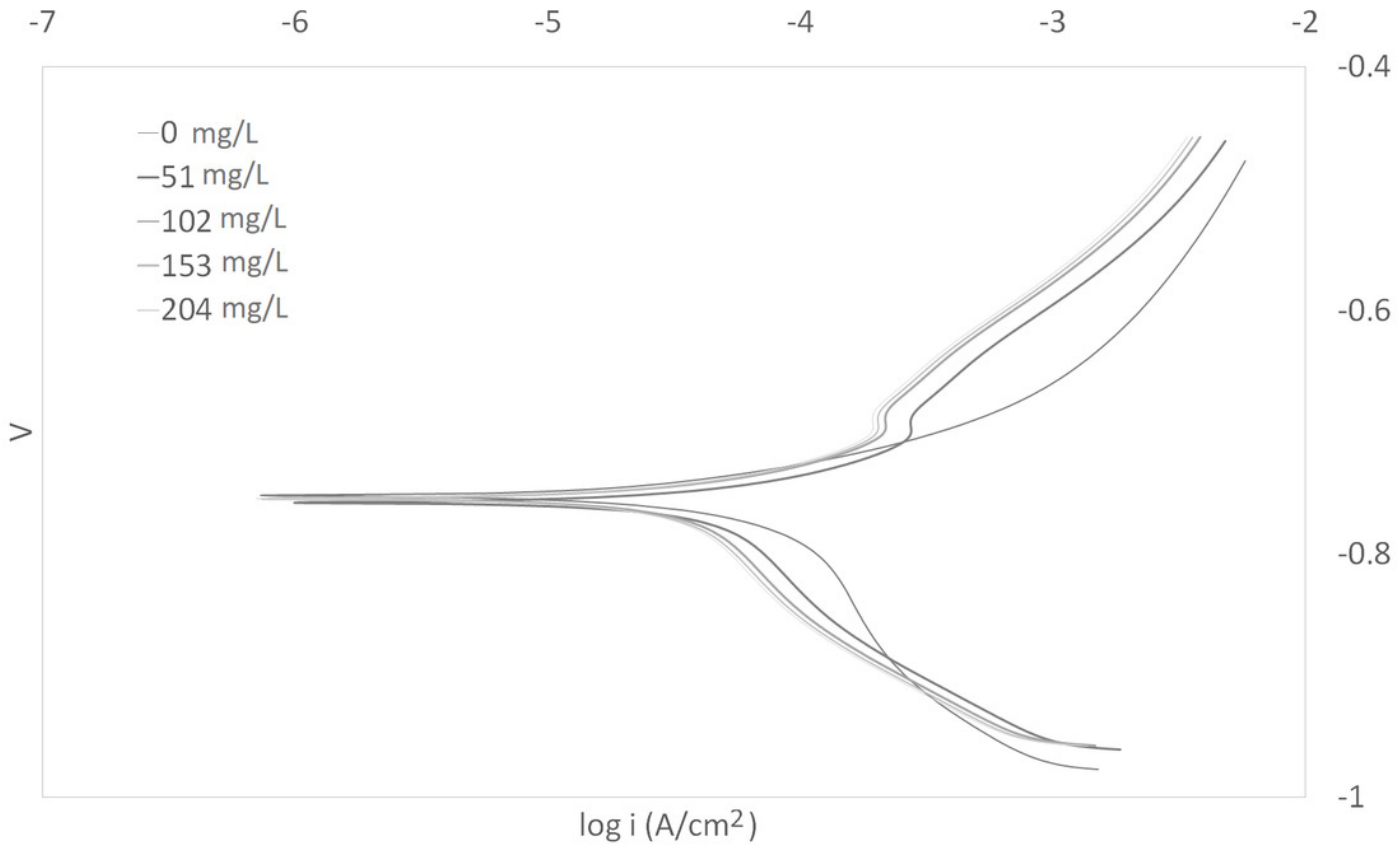

Figure 3

Tafel plot for carbon steel in 3.64% NaCl concentrated with CO_2 with different concentrations of synthetic EPS at 70°C

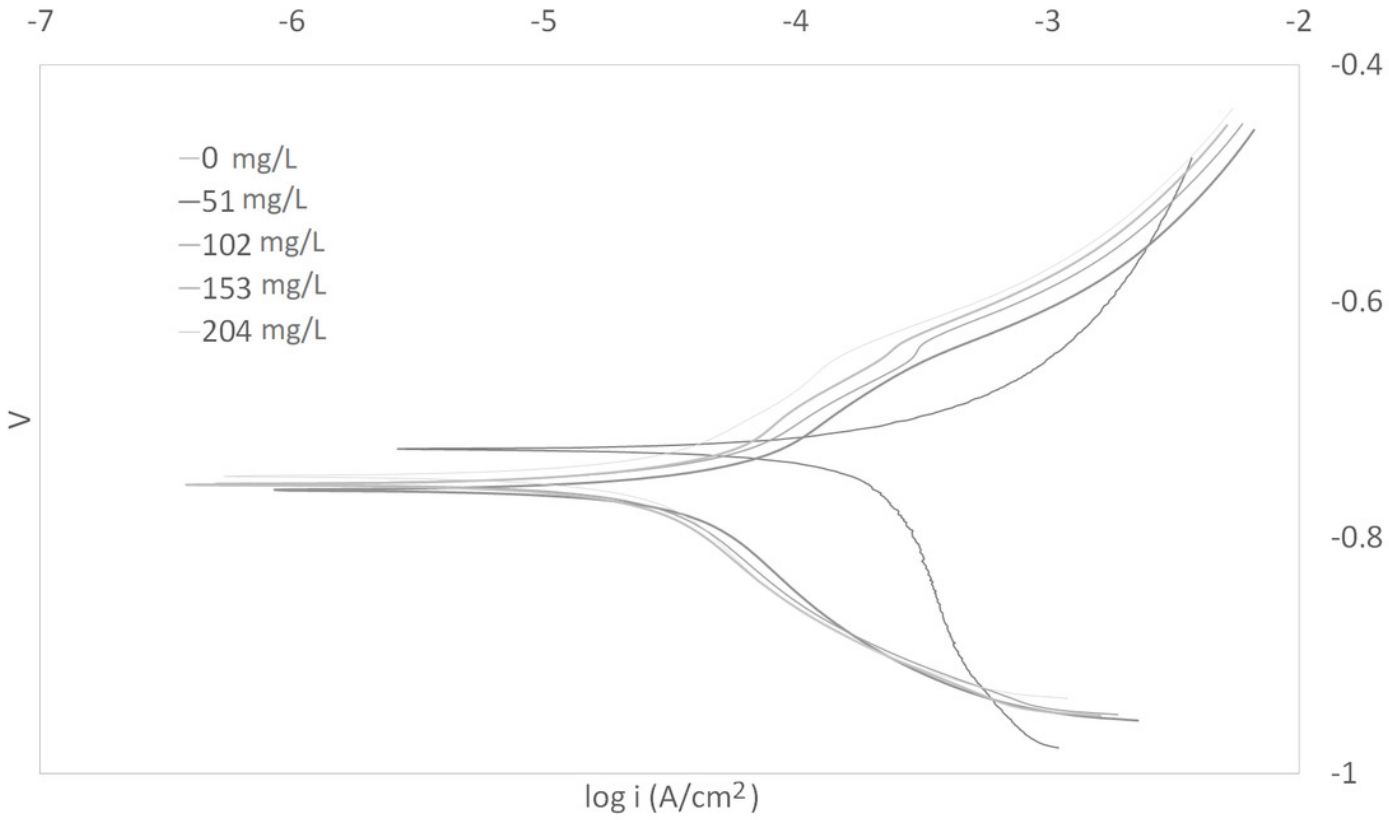

Figure 4

Arrhenius plots of ln I_{corr} versus 1/T at different concentrations of synthetic EPS

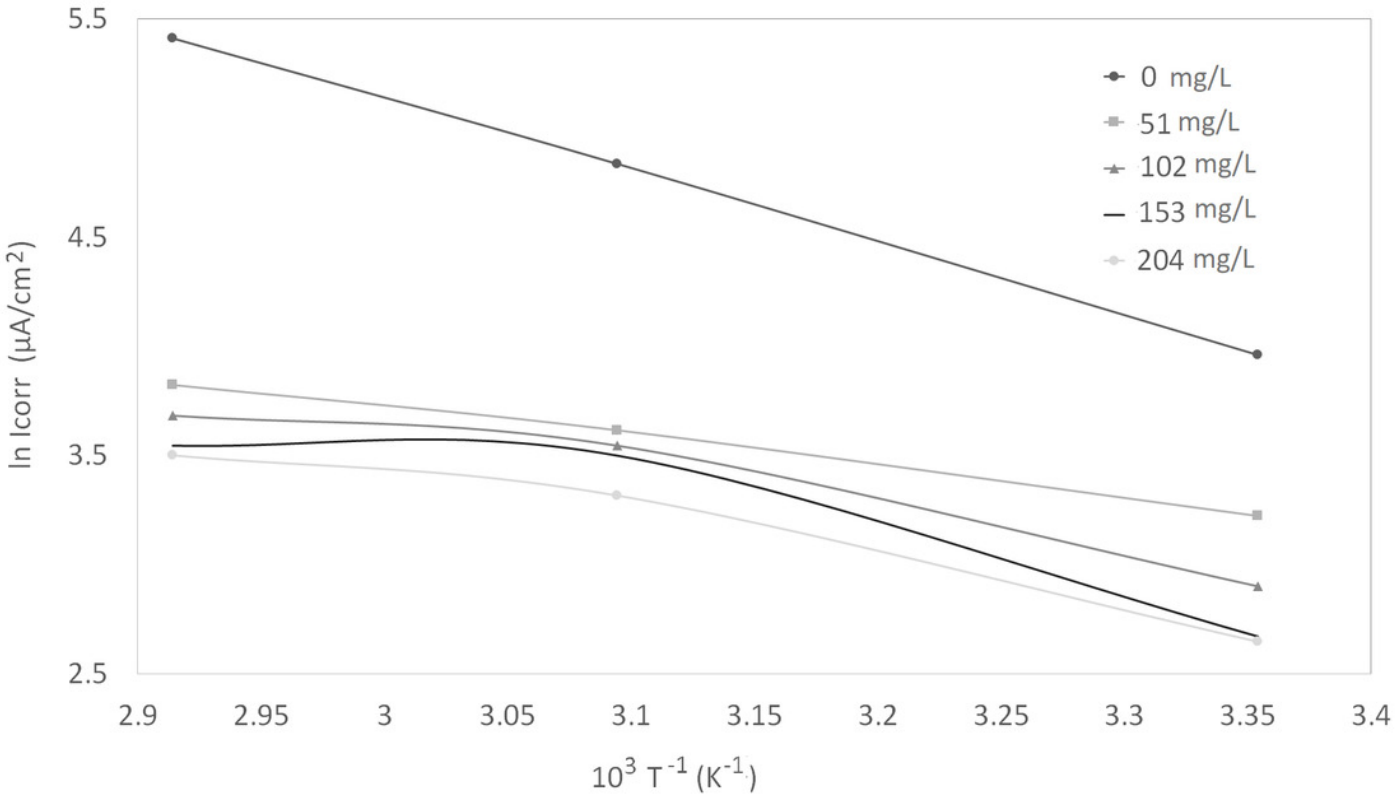

Figure 5

Arrhenius plots of corrosion ln (I_{corr}/T) versus 1/T at different concentrations of synthetic EPS

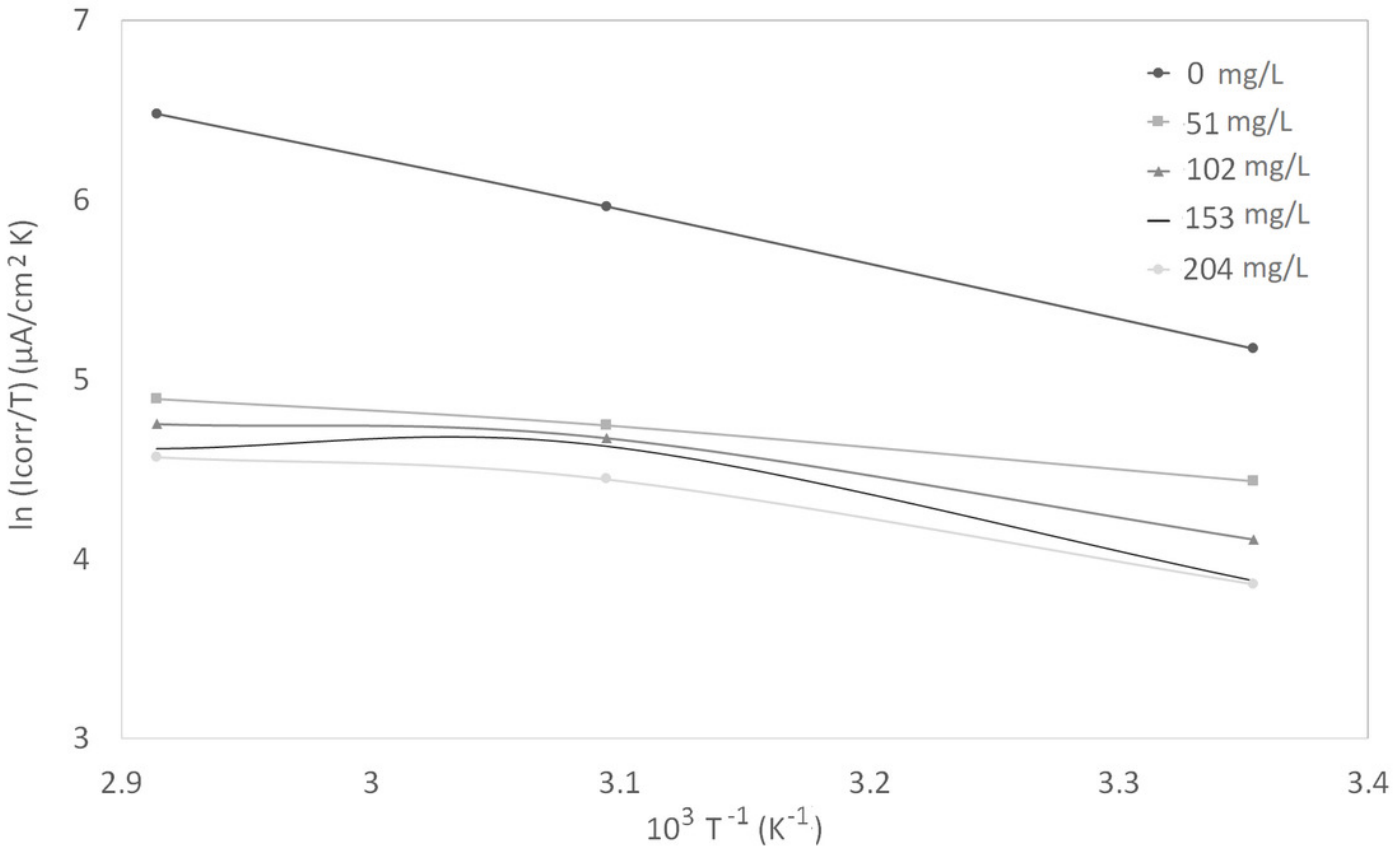

Figure 6

Curve fitting of the experimental data to Langmuir isotherm

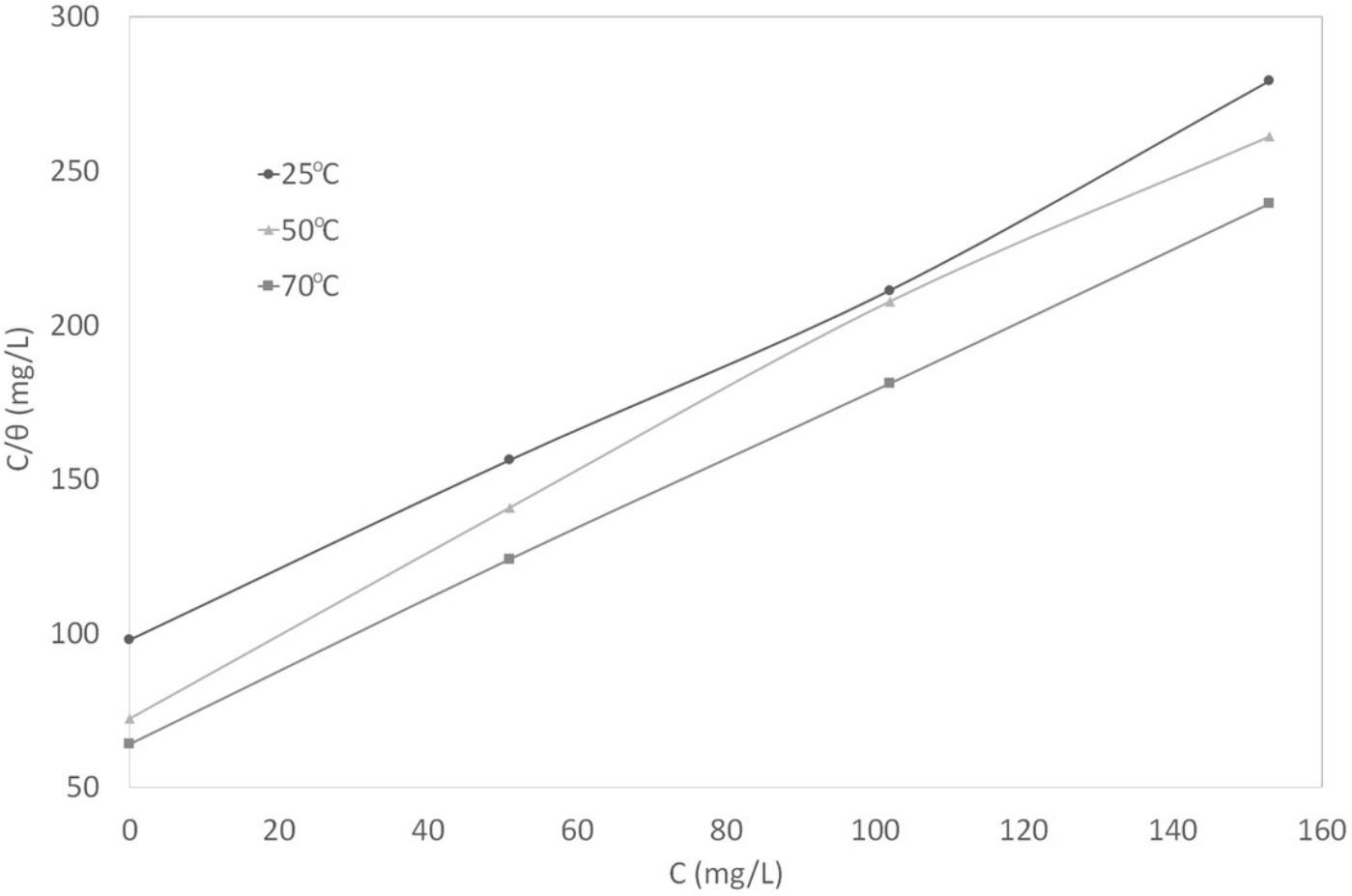

Figure 7

Van't Hoff plot

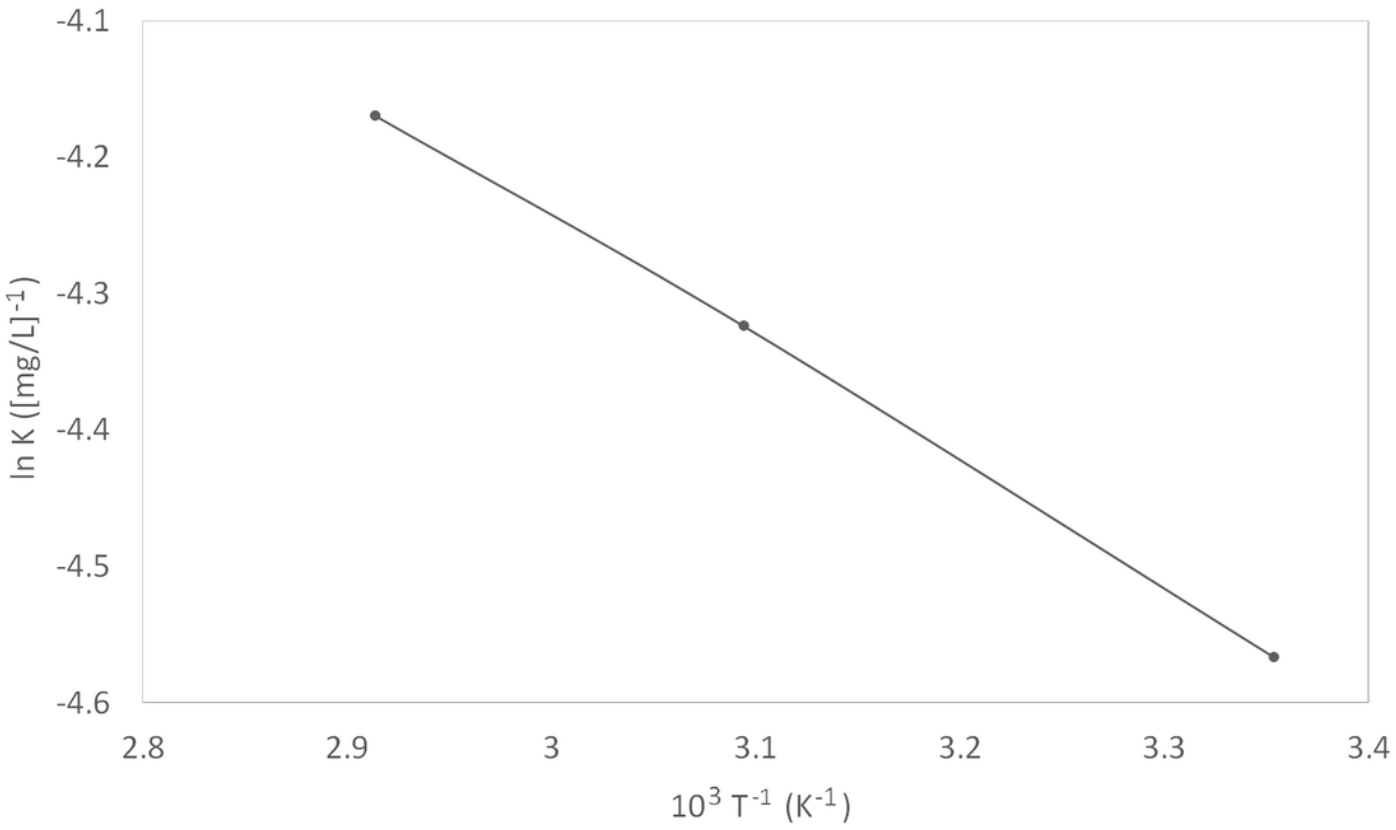

Figure 8

IR spectra of synthetic EPS

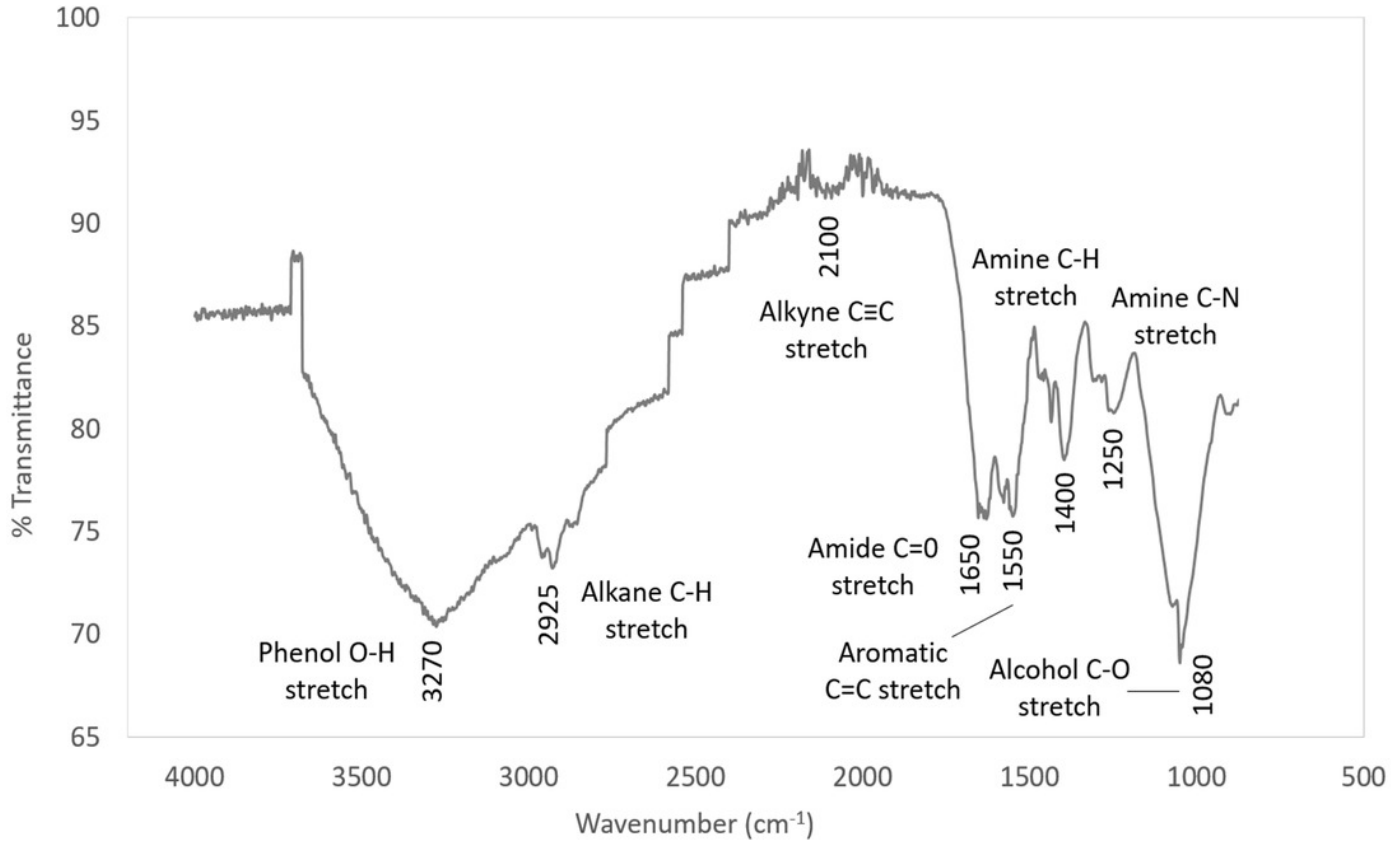

Figure 9

Chemicals in synthetic EPS and their structures